JOURNAL OF AGRICULTURAL AND FOOD CHEMISTRY

J. Agric. Food Chem. **2003,** *51,* 211–217 **211**

The Question of High- or Low-Temperature Glass Transition in Frozen Fish. Construction of the Supplemented State Diagram for Tuna Muscle by Differential Scanning Calorimetry

VIBEKE ORLIEN, JENS RISBO,* MOGENS L. ANDERSEN, AND LEIF H. SKIBSTED

Food Chemistry, Department of Dairy and Food Science, Royal Veterinary and Agricultural University, Rolighedsvej 30, DK-1958 Frederiksberg C, Denmark

The thermal behavior of fresh tuna muscle, rehydrated freeze-dried tuna muscle, and tuna sarcoplasmic protein fraction was studied by three types of differential scanning calorimetry (DSC): conventional DSC, alternating DSC, and sensitive micro-DSC. The relationship between glass transition temperature, T_g, and water content was established. Only a low-temperature glass transition was detected for fresh tuna and freeze-dried tuna rehydrated to high water contents, whereas for sarcoplasmic protein fraction both a low-temperature and an apparent high-temperature glass transition were detected for samples of high water content. Construction of the supplemented state diagrams for whole tuna muscle and for tuna sarcoplasmic protein fraction confirmed the low-temperature transition to be glass transition of the maximally freeze-dehydrated phase. The apparent upper transition of sarcoplasmic protein fraction was shown not to be a glass transition but rather to originate from the onset of melting of ice, and the temperature of this event should be denoted T_m'. The glass transition temperature and the concentration of the maximally freeze dehydrated tuna muscle are −74 °C and 79% (w/w), respectively.

KEYWORDS: Glass transition; differential scanning calorimetry; state diagram; glass relaxation; ice melting; frozen fish

INTRODUCTION

The hypothesis that food stability is dramatically influenced by significant changes in mechanical properties associated with glass transitions has been the subject of numerous investigations. Several studies have dealt with the consequences of the physical state of dried glassy systems for deteriorative chemical reactions in food systems (*1*−*6*). In systems with a high water content, the glass transition temperature is situated below the equilibrium ice freezing temperature, T_m, and for these systems the interplay between ice and glass formation can be characterized by supplemented state diagrams (*7*), which describe the different phases and the changes in physical state at various temperatures and water contents. In relation to frozen storage, two temperatures are characteristic for such systems: The glass transition temperature of the maximally freeze-dehydrated dry matter (for solutions often called maximally freeze concentrated), T_g', and the lower temperature boundary for equilibrium ice formation, T_m' (*7*). Regarding frozen storage, it is commonly accepted that T_g' is the relevant glass transition temperature for increased storage stability (*8*−*12*), since commercial freezing of food often is a relatively slow process, which allows for nearly maximum ice formation.

Historically, the thermal events observed in differential scanning calorimetry thermograms associated with T_g' and T_m' have been misinterpreted in terms of lower and upper glass transitions (*13*). Whereas the issue of double glass transitions has been clarified for simple systems of carbohydrate solutions (*14*, *15*), the existence of either a high, a low, or both types of T_g' in fish muscle is still a matter of controversy and a subject of investigation (*16*−*20*). Precise knowledge of the glass transition properties of freeze-dehydrated dry matter of fish is mandatory if the hypotheses of the effect of glass transition on storage stability is to be tested by studying how the stability of fish depends on the temperature during frozen storage.

In this paper, we describe the construction of supplemented state diagrams for tuna muscle and tuna sarcoplasmic protein fraction as a method for studying the glass transition properties of tuna muscle and for discussing the question of multiple glass transitions in fish muscle in general. Tuna muscle samples of various water contents was prepared by freeze-drying and rehydration to preset water activities, and the thermal behavior of the samples was studied by differential scanning calorimetry. In this way, the consistency between glass transition temperatures in samples without ice formation and samples with ice formation was studied, and possible T_m'-related phenomena can be distinguished from real glass transitions. The results presented

* To whom correspondence should be addressed (telephone +45 3528 3224; fax +45 3528 3344; e-mail jri@kvl.dk).

10.1021/jf020355x CCC: $25.00 © 2003 American Chemical Society
Published on Web 11/23/2002

Table 1. Calorimetry Protocol[a]

temperature[b] (symbol)[c]	calorimetry	β (°C/min)	anneal[d]	A_T (°C)	p (min)
$T_{g,o}$ (◆), $T_{g,e}$ (◇)	DSC	10	–	–	–
$T_{g,o}'$ (×), $T_{g,e}'$ (+), T_m' (▽)	DSC	10	–40 °C, 420 min[e] –50 °C, 45 min[f] –50 °C, 180 min[g]	–	–
$T_{g,o}$ (⊕), $T_{g,e}$ (⊗)	ADSC	1	–	1	1
$T_{g,o}$ (□), $T_{g,e}$ (○)	MicroDSC	1	–	–	–

[a] All samples were loaded onto the DSC instruments at 25 °C and then cooled to an appropriate temperature, followed by a heating segment as tabulated. [b] $T_{g,o}$, onset temperature; $T_{g,e}$, endset temperature. [c] The symbols refer to **Figures 4** and **6**. [d] Annealing procedure: after the cooling segment, the sample was heated to the annealing temperature and held for the given time. [e] Tuna muscle samples. [f] 50% and 66.7% sarcoplasmic protein fraction. [g] 20% sarcoplasmic protein fraction.

in this paper furthermore contribute to the scarce literature on state diagrams of real food systems (*21*).

MATERIALS AND METHODS

Fish Samples. Tuna muscle was obtained from a local retailer and used fresh or stored at −18 °C until use. The water content of the tuna samples was adjusted by the following procedure. Tuna muscle was freeze-dried for 24 h in an Edwards laboratory freeze-dryer at 0.1 mbar with the condenser operating at −50 °C. The freeze-dried tuna samples were subsequently stored in an evacuated desiccator over P_2O_5 (relative humidity 0.0%) for further dehydration. The dried tuna samples were transferred to desiccators and stored at room temperature until equilibrium over saturated salt solutions of LiCl, $MgCl_2 \cdot 6H_2O$, K_2CO_3, $Mg(NO_3)_2 \cdot 6H_2O$, NaBr, $SrCl_2 \cdot 6H_2O$, NaCl, KBr, KCl, $BaCl_2 \cdot 2H_2O$, or K_2SO_4. The water content of the rehydrated freeze-dried sample, the dry sample (stored over P_2O_5), and the fresh tuna muscle was determined by incubating samples of 0.01−0.02 g in 5 mL of dry methanol (<0.005% water) for 24 h and subsequently determining the water content of 1 mL of the methanol suspension by Karl-Fischer titration (Mettler DL18, Schwerzenbach, Switzerland). Freeze-dried sample rehydrated to the water content of fresh tuna was prepared by adding the appropriate amount of water to dry tuna.

Sarcoplasmic Protein Fraction. The procedure of Brake and Fennema (*20*) was used for isolating water-soluble sarcoplasmic proteins. The isolated sarcoplasmic protein fraction, which may have a content of low-molecular-weight salts and sugars, was freeze-dried and then rehydrated to different water contents with water to give a content of either 20% dry matter (w/w) or 50% dry matter (w/w), or rehumidified at room temperature to preset water activities over saturated solutions of LiCl, $MgCl_2 \cdot 6H_2O$, $Mg(NO_3)_2 \cdot 6H_2O$, or NaCl. The water content of the rehydrated samples was determined by Karl-Fischer titration as described above.

Differential Scanning Calorimetry. The thermal behavior of the samples was studied by three types of differential scanning calorimetry: conventional differential scanning calorimetry (DSC), alternating DSC (ADSC), and sensitive micro-DSC (MicroDSC). The specific protocols varied with the sample type and method of calorimetry. Details of the calorimetric protocols are given in **Table 1**. In general, glass transition was associated with the endothermic baseline shift. The onset and the endset temperatures of the transitions were determined as the intersection points of the tangents to the heat flow curve step and to the pre- and post-step baselines using the DSC software packages supplied with the instruments.

Conventional DSC. The conventional DSC experiments were performed with a DSC 820, Mettler Toledo (Schwerzenbach, Switzerland), which is based on the heat flux principle and cooled with liquid nitrogen. The heat flow and temperature were calibrated with indium (T_m = 156.6 °C, ΔH_{fus} = 28.5 J/g) and zinc (T_m = 419.5 °C, ΔH_{fus} = 107.5 J/g) as standards. The low-temperature calibration was checked with decane (T_m = −29.66 °C) and cyclohexane (T_m = 6.47 °C). Samples of tuna muscle (10−20 mg) and sarcoplasmic protein fraction (10−20 mg) were weighed, hermetically sealed in 40 μL aluminum DSC crucibles, and scanned over an appropriate temperature range with the heating scan rate β (linear up-scan), using an empty crucible as reference.

Alternating DSC. For the ADSC technique, the same heat flux DSC instrument used for conventional DSC was used, but an oscillating heating profile was applied, combined with a conventional linear up-scan (*22*−*24*). The heating profile is characterized by the heating rate (β) of the underlying temperature ramp and the period (p) and amplitude (A_T) of the oscillating temperature modulation.

Sensitive MicroDSC. Improved sensitivity and thus easier detection of glass transition in dry tuna muscle was achieved by MicroDSC experiments using a Micro DSC III calorimeter, SETARAM (Caluire, France), with water as external cooling medium. Calibration of heat flow and temperature was performed with naphthalene (T_m = 80.3 °C, ΔH_{fus} = 145.5 J/g). An aliquot of ∼120 mg of sample was transferred to an inert metal vessel and hermetically closed. Samples were scanned over an appropriate temperature range with an empty vessel as reference.

Annealing Optimization. Optimization of the annealing procedure for samples with high water content was performed using the conventional DSC technique and involved self-consistently applying an isothermal annealing at a temperature between the resulting T_g' and T_m'. Annealing in this temperature interval promotes maximal ice formation and is recommended in the literature (*27*). Optimization of the annealing procedure involved the following steps:

(i) An initial linear up-scan was performed without annealing for determination of the preliminary T_g' and T_m' values.

(ii) New T_g' values were determined by two or three scans after a 30 min annealing period at various temperatures above the preliminary T_g' and preferably close to the preliminary T_m'.

(iii) The next annealing temperature was selected above the highest T_g determined in the previous scans, and still not exceeding T_m'. New scans were performed after a longer annealing period of 60 or 120 min.

(iv) The isothermal annealing period was increased until no change in the observed glass transition occurred, and the observed glass transition temperature was then interpreted as T_g'.

Nonlinear fitting was performed by a Levenberg−Marquardt scheme using Microcal Origin software, version 6.

RESULTS

Tuna. Thermograms of fresh tuna muscle obtained by conventional DSC protocol revealed two characteristic thermal events: the glass transition and the ice melting (**Figure 1**). The thermogram of non-annealed tuna showed a broad glass transition temperature range beginning at $T_{g,o}$ = −80 °C and ending at $T_{g,e}$ = −62 °C (**Figure 1A**). At higher temperatures, an endotherm associated with melting of ice was observed (**Figure 1B**,**C**). As shown by tangent construction in **Figure 1B**, the melting of ice started at T_m' = −29 °C. The onset of ice melting gives rise to a feature in the thermogram that is similar to a baseline shift immediately followed by a melting endotherm. Due to the relatively large amount of heat involved, together with a finite scanning rate and finite calorimeter response time (*25*), the ice melting ended at an apparent T_m above 0 °C (**Figure 1C**). The optimized annealing procedure (cf. Materials and Methods) for fresh and rehydrated tuna was found to be 420 min at −40 °C. For fresh tuna, the annealing procedure resulted in a glass transition at a higher temperature with an onset temperature at $T_{g,o}'$ = −74 °C and an endset temperature at $T_{g,e}'$ = −56 °C (**Figure 1A**). Additional experiments using annealing at −50 °C for 420 min gave equivalent glass transition temperatures. Experiments on thawed samples stored in a freezer and freeze-dried samples rehydrated to the water content of fresh tuna showed that the glass transition properties were left unchanged by the freezing and freeze-drying processes. Also, when using the same annealing procedure, DSC

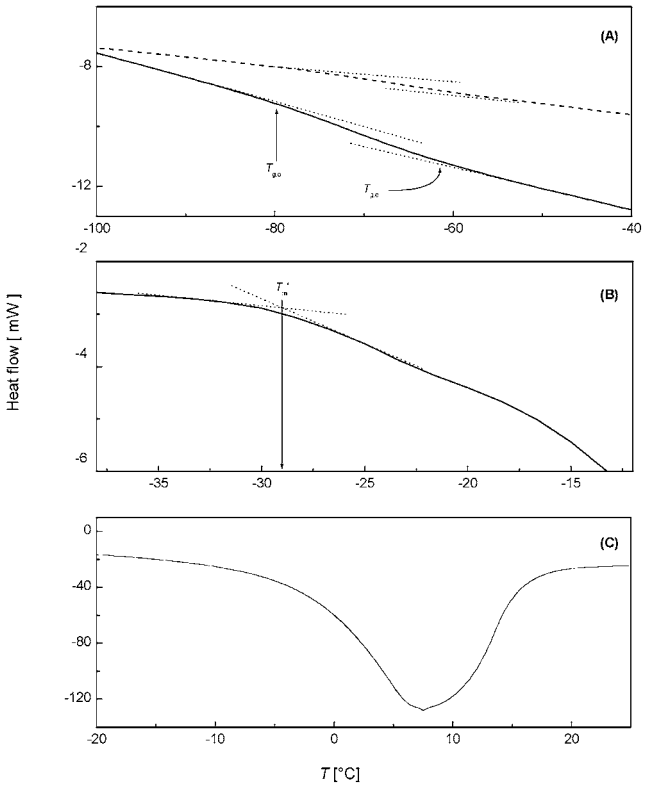

Figure 1. Thermograms of fresh tuna muscle obtained by DSC experiments, as described in **Table 1**. (A) The low-temperature part of the thermograms of annealed and non-annealed samples. The heat flow curve of non-annealed tuna (—) shows a glass transition range from –80 to –62 °C, denoted $T_{g,o}$ and $T_{g,e}$, respectively. For the annealed sample (– –), the glass transition range is from –74 to –56 °C. (B) The medium-temperature part of an annealed sample. The onset of ice melting at $T_m' = -29$ °C is indicated by tangents to the heat flow curve. (C) The high-temperature part of the thermogram for a sample. The melting endotherm ends at a temperature above 0 °C.

scans of the freeze-dried tuna rehydrated to lower water contents of 22.5−47.4% (w/w): almost identical glass transition ranges (cf. **Table 2**) and onset of ice melting temperatures were observed. Also for these rehydrated tuna samples with lower water content, the glass transition temperatures of non-annealed samples were considerably lower, as can be seen in **Table 2**. The ice melting endotherm was systematically smaller for samples of lower water content.

Thermograms obtained by DSC of freeze-dried samples rehydrated to lower water contents (9.4−21.42%) did not display an ice melting endotherm and further revealed that the glass transitions occurred at higher temperature ranges with decreasing water contents. The results from the conventional calorimetry experiments with fresh and rehydrated tuna are summarized in **Table 2**.

Glass transitions could not be identified by the conventional linear scan protocol (DSC) for freeze-dried samples that had been rehydrated to water contents lower than about 9% (w/w), and the more sensitive MicroDSC and ADSC techniques were therefore employed. **Figure 2** shows results from a MicroDSC experiment on a rehydrated sample with water content of 3.49% (w/w). In the thermogram of **Figure 2**, a glass transition range from $T_{g,o} = 40$ °C to $T_{g,e} = 54$ °C, accompanied by a glass relaxation, can be identified. As the glass temperature was above room temperature, these dry samples had, in contrast to the more wet samples, been stored in a glassy state during the full rehydration period and during handling before the calorimetric

Table 2. Water Contents of Fresh and Rehydrated Freeze-Dried Tuna Samples and Glass Transition Temperature Obtained by Various Calorimetric Methods

a_w[a]	water content, % (w/w)	$T_{g,o}$ (°C)	$T_{g,e}$ (°C)	calorimetry[b]
0.00	1.86	51	62	MicroDSC
		71	110	ADSC
0.11	3.49	40	54	MicroDSC
		53	69	ADSC
0.33	6.21	2	45	ADSC
0.43	6.76	–10	41	ADSC
0.527	9.38	–19	–5	DSC
		–20	30	ADSC
0.577	10.35	–31	–10	DSC
0.712	14.64	–55	–27	DSC
0.76	16.32	–60	–40	DSC
0.81	21.42	–72	–52	DSC
0.842	22.5	–82	–59	DSC
		–74 ($T_{g,o}'$)	–52 ($T_{g,e}'$)	DSC, anneal
0.903	28.22	–93	–62	DSC
		–74 ($T_{g,o}'$)	–53 ($T_{g,e}'$)	DSC, anneal
0.975	47.35	(–90)[c]	(–61)[c]	DSC
		–76 ($T_{g,o}'$)	–60 ($T_{g,e}'$)	DSC, anneal
(with water)	70.4	–74 ($T_{g,o}'$)	–55 ($T_{g,e}'$)	DSC, anneal
(fresh)	70.4	(–80)[c]	(–61)[c]	DSC
		–74 ($T_{g,o}'$)	–55 ($T_{g,e}'$)	DSC, anneal
water	100	–137	–125	from (*29*)

[a] Water activity at 25 °C (*33*, *34*). [b] Refers to **Table 1**. [c] Not compiled into **Figure 4**.

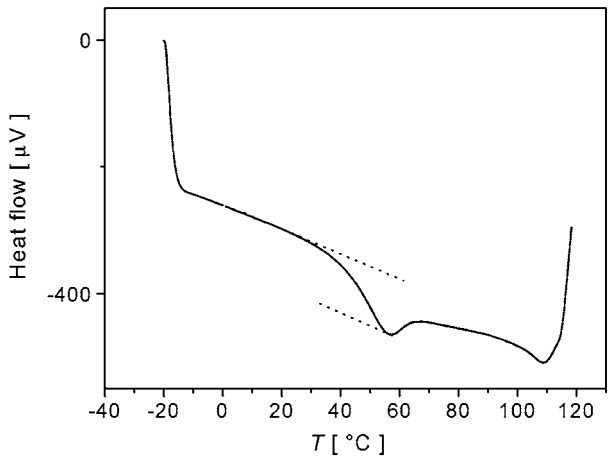

Figure 2. MicroDSC thermogram of a rehydrated freeze-dried tuna sample with water content of 3.49% (w/w). A glass transition range with $T_{g,o} = 40$ °C and $T_{g,e} = 54$ °C is observed. Superimposed on the glass transition, a glass relaxation can be identified.

experiment, thus presumably giving rise to the observed relaxation phenomenon, which is caused by relaxation of the glass to a state of lower enthalpy during aging of the glass (*26*).

With ADSC, it was possible to separate the detected heat flow into two components: the heat capacity-related (reversing) heat flow, and the kinetic (non-reversing) heat flow contributions (*22*, *23*). The non-reversing heat flow is caused by processes which are not reversible within the time scale of one period of the sinusoidal modulation, or by truly irreversible processes such as oxidative degradation of the sample or crystallization of amorphous material (*22*−*24*). Processes which are thermodynamically reversible within a modulation period cause events observed in the reversing heat flow such as glass transitions (*22*−*24*). The resulting three different heat flow curves for a rehydrated freeze-dried tuna sample with water content of 6.21% (w/w) are shown in **Figure 3**. Inspection of the total heat flow curve did not reveal a glass transition, since no baseline shift

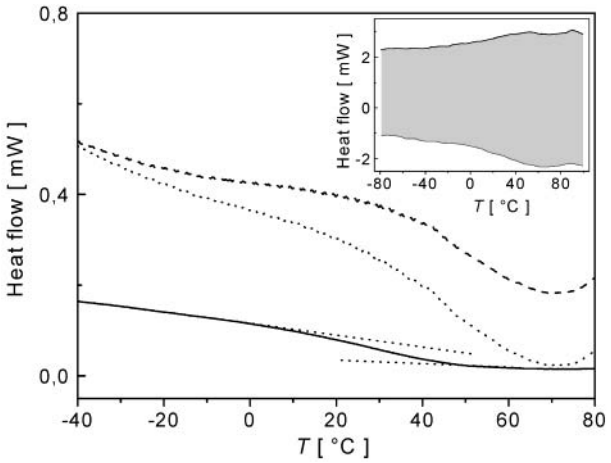

Figure 3. ADSC thermogram of a rehydrated freeze-dried sample with a water content of 6.21% (w/w). The total heat flow curve (– –) is separated into two components: the non-reversing heat flow (• • •) and the reversing heat flow (—). In the reversing heat flow curve, a glass transition with $T_{g,o} = -10$ °C and $T_{g,e} = 41$ °C can be identified. Inset: The alternating heat flow envelope ADSC from which the total reversing and non-reversing heat flow curves are generated.

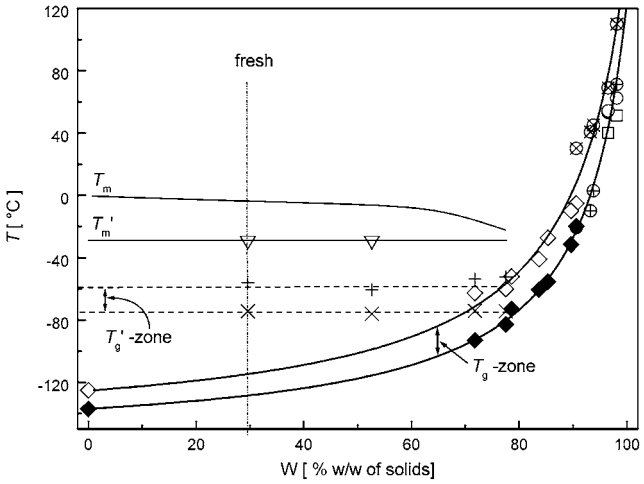

Figure 4. Supplemented state diagram for the system of tuna solids and water, as constructed from calorimetric experiments on fresh and rehydrated freeze-dried tuna. Symbols refer to the calorimetric schemes summarized in **Table 1** and calorimetric results summarized in **Table 2**. The T_g lines interpolate the DSC and ADSC data and are drawn using the Gordon–Taylor equation, as described in the text. The T_m line is only drawn for completeness of the diagram and is not based on actual experiments.

was detected. However, when the non-reversing heat flow was discarded and the reversing heat flow curve was inspected, a rather broad glass transition range with $T_{g,o} = -10$ °C and $T_{g,e} = 41$ °C was observed.

The results of all the calorimetric experiments on fresh and rehydrated whole tuna muscle are summarized in **Table 2** and presented in **Figure 4** as a supplemented state diagram. **Table 2** facilitates a comparison of glass transition temperatures obtained by the various calorimetric methods in order to deduce the mutual consistency of the methods. The glass transition temperature of tuna samples rehydrated to a water content of 9.38% (w/w) is reported both from DSC and ADSC experiments. It is seen that the two methods give equivalent $T_{g,o}$ values of −19 and −20 °C, and it is therefore concluded that the two methods are mutually consistent with respect to onset temperatures. This is not the case for the $T_{g,e}$ values, as the transition

Table 3. Water Contents and Glass Transition Temperatures for Sarcoplasmic Protein Fraction

a_w[a]	water content, % (w/w)	$T_{g,o}$ (°C)	$T_{g,e}$ (°C)	calorimetry[b]
0.00	0	62	76	DSC
0.11	4.38	27	42	DSC
0.33	9.36	–6	7	DSC
0.527	16.2	–38	–28	DSC
0.76	33.28	–82	–72	DSC
		–69 ($T_{g,o}'$)	–59 ($T_{g,e}'$)	DSC, anneal
(with water)	50	–67 ($T_{g,o}'$)	–57 ($T_{g,e}'$)	DSC, anneal
(with water)	20	–67 ($T_{g,o}'$)	–58 ($T_{g,e}'$)	DSC, anneal

[a] Water activity at 25 °C (*33*, *34*). [b] Refers to **Table 1**.

range observed with ADSC in general is much broader (40−50 °C) than the one observed with DSC (about 20 °C). Therefore, most emphasis should be given to the glass transition onset temperatures of the state diagram, **Figure 4**.

For rehydrated samples of 1.86% and 3.49%, it was possible to compare the MicroDSC and the DSC methods. From **Table 2** it can be seen that the $T_{g,o}$ values of MicroDSC are 13−20 °C lower than the ones observed with ADSC, and it is therefore concluded that the two methods are not fully consistent. As ADSC is compatible with DSC, we chose to use the MicroDSC results in a more qualitative way. Due to the narrow and well-defined transition region, the MicroDSC results serve merely as supplementary proof of a glassy state in tuna systems of low water content.

The annealing protocol used in this study ensures that the observed glass temperatures of fresh tuna are independent of the annealing time when the annealing time is longer than 420 min and independent of annealing temperature for annealing temperatures between the observed glass transitions temperature and the onset of ice melting. The facts indicate that the annealing procedure used in this study produces a maximally freeze-dehydrated state in fresh tuna and that the observed glass transition temperatures should be interpreted as T_g' values.

The fact that fresh tuna and samples rehydrated to the same water content gives the same glass transition temperatures justifies that the glass transition properties of tuna of low water content can be studied using freeze-dried samples. The glass transition temperatures of annealed rehydrated samples and annealed fresh tuna forms, together a concentration-independent T_g' zone, as can be seen in **Table 2**, and as indicated in **Figure 4** with horizontal lines. The finding of a concentration-independent T_g' zone strongly supports the interpretation of a maximally freeze-dehydrated state in frozen fresh tuna and rehydrated tuna with the $T_{g,o}'$ value of the tuna solids and water system of about −74 °C.

The intersection of the horizontal T_g' line and the T_g line provides the concentration of the maximally freeze-concentrated glass, C_g', which in the case of tuna muscle is 79% (w/w), as determined from **Figure 4**. The glass transition temperature ranges observed by the various calorimetric schemes in non-annealed samples, together with the glass transition temperature of water (*28*, *29*), form a continuous T_g zone, as can be seen in **Figure 4**. The boundaries of this zone are interpolated by fitting the Gordon−Taylor equation (*35*) to the DSC and ADSC onset and completion temperatures using the glass transition of completely dry tuna solids and the weighting factor, *k*, as free parameters. The results of the two fitting procedures are summarized in **Table 4**. The T_m line of the state diagram, shown in **Figure 4**, is drawn only for completeness of the diagram and is not based on actual experiments.

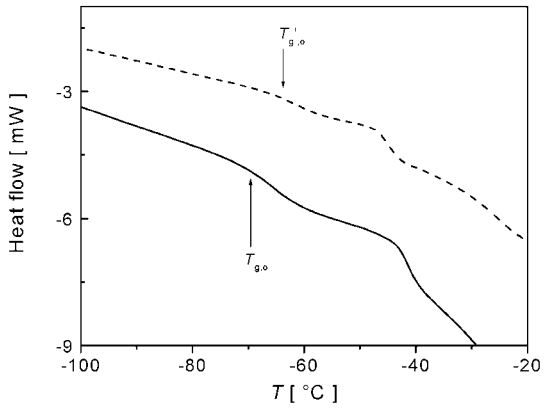

Figure 5. Conventional linear up-scan (DSC) thermograms of 20% (w/w) solutions of sarcoplasmic proteins obtained with (– –) and without (—) annealing. The scanning and annealing protocol is summarized in **Table 1**. The glass transition range of the non-annealed sample is –72 to –61 °C, and that for the annealed sample is –67 to –58 °C.

Table 4. Gordon–Taylor Parameters Obtained by Nonlinear Fitting to Calorimetric Data

	$T_{g,o}$ (°C)	$T_{g,c}$ (°C)	k onset	k completion
tuna muscle	124 ± 8	154 ± 14	12.4 ± 0.8	10.5 ± 1.2
sarcoplasmic protein fraction	–	–	5.1 ± 0.09	5.3 ± 0.2

Sarcoplasmic Proteins. Water-soluble sarcoplasmic proteins were isolated from tuna muscle in order to further investigate the potential glass forming fractions of the tuna dry matter. A limited number of conventional calorimetric experiments were performed with samples of sarcoplasmic proteins that had been freeze-dried and rehydrated to different water contents. **Figure 5** shows thermograms of annealed and non-annealed 20% w/w solutions of the sarcoplasmic protein fraction. The scanning and annealing protocols are summarized in **Table 1**. The non-annealed sample showed a glass transition range from $T_{g,o} = -72$ °C to $T_{g,e} = -61$ °C, whereas annealing raised the glass transition range from $T_{g,o}' = -67$ °C to $T_{g,e}' = -58$ °C. At higher temperatures, a large endothermic baseline shift was observed for both kinds of samples; the origin of this "upper" transition will be discussed below. Similar glass transition ranges were observed for DSC scans of sarcoplasmic protein rehydrated to 50% and 66.7% (w/w) when the same annealing protocol was applied, although shorter annealing periods were needed in order to obtain a consistent glass transition temperature. Similar to the case for tuna muscle, the glass transition ranges occurred at higher temperatures with samples with lower water contents. The results of the calorimetric experiments on samples with various water contents are summarized in **Table 3** and presented in **Figure 6** as a supplemented state diagram for the system of pseudobinary mixtures of tuna sarcoplasmic proteins and water. The T_g lines were interpolated by fitting the weighting factor, k, of the Gordon−Taylor equation to the onset as well as completion temperatures obtained by calorimetry (cf. **Table 4**). From **Figure 6** it is seen that the maximally freeze-concentrated state is characterized by a $T_{g,o}'$ of −67 °C and a water content of about 25% (w/w).

DISCUSSION

It has been hypothesized that the glass transition of the maximally freeze-concentrated phase (T_g') should act as a temperature threshold for the stability of frozen foods. Notable in this context, no general annealing optimization protocol for determining T_g' has been reported before. In the present calorimetric study, we have employed a general "self-consistent" annealing procedure, which involves multiple DSC trial scans in order to determine a proper annealing temperature between T_g' and T_m'. The procedure furthermore involves determination of the annealing times that are adequate for obtaining consistent glass transition temperatures.

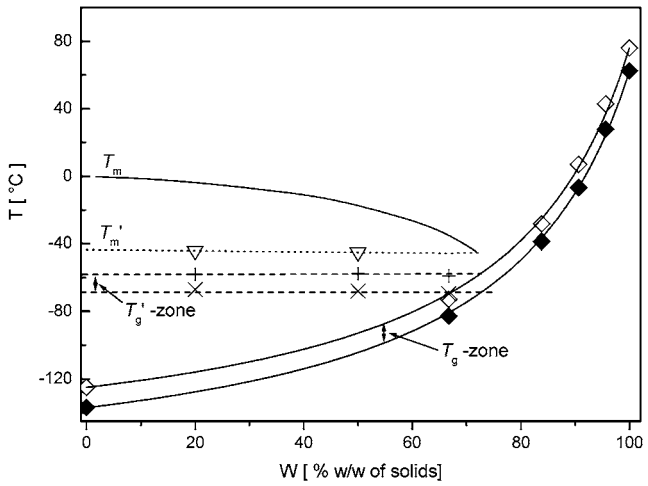

Figure 6. Supplemented state diagram of the pseudobinary system of sarcoplasmic protein fraction and water, as constructed from DSC experiments. Symbols refer to the calorimetric schemes summarized in **Table 1** and calorimetric results summarized in **Table 3**. The T_g lines are interpolated using the Gordon–Taylor equation as described in the text. The T_m line is only drawn for completeness of the diagram and is not based on actual experiments.

Using optimized annealing procedures, low-temperature glass transitions of fresh/rehydrated tuna muscle and the sarcoplasmic protein fraction were detected at $T_{g,o}' = -74$ °C and $T_{g,o}' = -67$ °C, respectively. These glass transition temperatures were independent of the water content for annealed samples, and thus we interpret this transition to be the glass transition of the maximally freeze-dehydrated phase.

The finding of a low-temperature glass transition of tuna muscle is in agreement with the low glass transitions reported for tuna, $T_g = -71$ °C (*16*), and cod, $T_g = -77$ °C (*17*, *18*). The fact that the glass transition temperatures for both the sarcoplasmic protein system and the tuna system at various water contents could be mapped into state diagrams (**Figures 4** and **6**) with the same structure as state diagrams of well-known glass-formers such as various sugars (*27*, *30*) strongly strengthens the interpretation of the low transition to be a true glass transition, with components present in the sarcoplasmic protein fraction as the main glass-former of the tuna.

An apparent "high" glass transition around −20 °C has been suggested for cod (*13*, *20*) and mackerel and sarcoplasmic proteins of mackerel (*20*), as an endothermic baseline shift was seen in this temperature range. In this study, an endothermic baseline shift has been detected around −45 °C (**Figure 5**) for samples of sarcoplasmic proteins with a water content high enough to make ice formation possible. However, these apparent second-order transitions were not observed in samples of lower water content, and therefore it is more likely that these features of the thermograms are associated with the presence of ice in the system. From the point of view of the state diagram, there is no W-dependent T_g line associated with the W-independent apparent T_g' line, where W is the concentration of dry matter.

Consequently, this apparent glass transition cannot be mapped into a state diagram of the well-known type. We take this as an indication that this "upper" transition of the sarcoplasmic protein fraction is not a glass transition in the common sense. The onset of ice melting at T_m' in annealed samples of fresh tuna gave rise to a transition with some similarity to an apparent "upper" glass transition. This may be related to the apparent findings of upper glass transitions in fish (*13*, *20*). These studies reported that an annealing temperature close to the apparent glass transition temperature was mandatory in order to observe the apparent "upper" glass transition at all or to observe the transition in a reproducible manner. As the tuna samples, in this study, were annealed at relatively low temperature, the finding of a less clear apparent "upper" glass transition is therefore not surprising in the light of the observation previously reported in the literature (*13*, *20*). The annealing procedure is usually taken to be related to ice formation on proper freeze concentration of the solids (*14*, *15*, *27*), and the annealing temperature is recommended to be higher than the glass transition temperature in order to ensure sufficient mobility of water but still low enough to ensure a driving force for further freeze concentration. A temperature in the interval of maximal ice formation is usually recommended to be optimal for annealing (*27*). The apparent upper glass transition temperature of fish was reported to be higher than the annealing temperature (*20*), and when the annealing temperature was changed in one direction, the apparent "upper" glass transition relocated in the same direction. This behavior is somehow different from the behavior seen for the well-studied glass-forming carbohydrate systems (*14*, *27*) and indicates that water is not immobilized in the apparent formed glass, as annealing at temperatures corresponding to the apparent glassy state seemed to increase freeze concentration. In the present study, only one glass transition was observed for the tuna samples of lower water contents, and this transition was related to the "low" T_g', as indicated in the state diagram, **Figure 4**. On the basis of the same arguments as used for sarcoplasmic proteins, we therefore suggest that the upper transition found for annealed fresh tuna is not related to glass formation.

Apparent double values of T_g have been encountered before in the low-temperature calorimetric studies of simple solutions of sugars and other carbohydrates (*13* and references therein). The lowest glass transition was interpreted to be the glass transition of incompletely freeze-concentrated domains of solution, whereas the upper transition was interpreted to be the glass transition of the maximally freeze-concentrated solution. This interpretation was inconsistent with the system of glycerol/water mixtures, where the two apparent transitions took place at widely separated temperatures, with the upper transition at a temperature higher than that of the glass transition of pure glycerol (*14*). The generally accepted interpretation is now that the lower transition is the glass transition of the freeze-concentrated solution (T_g') (*14*) and the upper apparent transition is due to the heat flow induced by the onset of ice melting at a temperature high enough to allow sufficient mobility. This temperature is now often denoted T_m' (*27*). We have established through various DSC experiments that the upper transitions of sarcoplasmic protein fraction and tuna are not actual glass transitions but rather events associated with the onset of ice melting. We therefore attribute this upper transition to the onset of ice melting and recommend the notation T_m'.

It has been suggested that the natural heterogeneity of biological material such as fish muscle and the inhomogenity due to molecular incompatibility in other complex food could explain multiple T_g values observed in these systems (*13*). However, the knowledge gained from model systems (*14*) the present results from experiments on sarcoplasmic proteins and tuna stress the importance of not "confusing" T_m' phenomena with actual glass transitions, as the onset of ice melting could be localized at specific temperatures and could give rise to an apparent endothermic baseline shift which easily can be misinterpreted in terms of a true glass transition.

A few comments are appropriate concerning the use of supplemented state diagrams as a description of complex materials, such as muscle food and multicomponent mixtures. A temperature/composition phase diagram is *N*-dimensional for an *N*-component mixture. From such a diagram, the composition and amount of any of the $N + 1$ possible phases can be read out. An example of constructing a map of the temperature dependence of a multicomponent system is the state diagram of the sucrose/glycine/water ternary system (*31*). For more than two components, such a diagram does not fit into the plane of the paper, and traditionally in the study of glass formation, examples have been seen of projection of a three-dimensional diagram for a fructose/glucose/water system onto a two-dimensional plane, which effectively describes the system as a two-component mixture of water and solids (*32*). In this process of projection, information on the higher dimensional space is lost; as a result, the solubility limit of solids is not well defined, as the two sugars are not equal, and information of the concentration of each of the sugars of a saturated solution cannot be determined from such a diagram. Concerning non-equilibrium freezing and glass formation, the situation is simpler, as the T_m line and the T_g line usually are interpreted as describing the coexistence of only two phases, pure water in the form of ice and a homogeneous concentrated solution; i.e., the molar ratio of the sugars in the solution is conserved, and no information is lost.

Concerning the more complex system, tuna muscle, the situation is different. Such biological materials are highly structured and heterogeneous, containing various cells, organels, and domains. For such materials, the T_m line and T_g line contain information about the average water content of the dehydrated materials coexisting with the ice formed in the system. Some parts of the freeze-concentrated solids may have higher water content and some parts lower water content. At a sufficiently low temperature, the combined effect of temperature and dehydration transforms parts of the solids into a glassy state. According to the state diagram, **Figure 4**, the average water content of the maximally dehydrated material is around 79% (w/w), with the possibility that the actual glassy parts have different and presumably lower water content.

In conclusion, the relationships between the glass transition temperature and water content of fresh tuna muscle and rehydrated tuna muscle (rehydrated to various water contents) were systematically investigated by three different differential scanning calorimetric techniques. To investigate the glass-forming part of tuna, the sarcoplasmic protein fraction was isolated from tuna muscle, and the dependence of the glass transition temperature on water content was observed with conventional DSC. The DSC results for both the tuna muscle and sarcoplasmic protein fraction were mapped into supplemented state diagrams. The construction of the supplemented state diagram for tuna muscle and tuna sarcoplasmic protein fraction confirms the existence of a glassy state in tuna. In relation to storage stability, the maximally freeze-concentrated glass transition temperature, T_g', and the related concentration, C_g', are the important parameters to be derived from the

supplemented state diagram. For tuna muscle and tuna sarcoplasmic protein fraction, these values are $T_{g,o}' = -74$ °C, $C_g' = 79\%$ and $T_{g,o}' = -67$ °C, $C_g' = 75\%$, respectively.

On the basis of the discussion of the question of a low- and a high-temperature glass transition, it may be concluded that the "upper" transition found for sarcoplasmic proteins and tuna is not a glass transition but, since it is observed only in samples with ice formation, is related to the onset of ice melting, and the temperature of this thermal event should be denoted T_m'. The results presented in this paper suggest that the apparent "upper" transition found in fish (*17*, *19*, *20*) should possibly be interpreted as the onset of ice melting instead of a glass transition.

LITERATURE CITED

(1) Orlien, V.; Andersen, A. B.; Sinkko, T.; Skibsted, L. H. Hydroperoxide formation in rapeseed oil encapsulated in a glassy food model as influenced by hydrophilic and lipophilic radicals. *Food Chem*. **2000**, *68*, 191−199.

(2) Brake, N. C.; Fennema, O. R. Lipolysis and Lipid oxidation in Frozen Minced Mackeral as Related to T_g', Molecular Diffusion, and Presence of Gelatin. *J. Food Sci.* **1999**, *64*, 25−32.

(3) Kerr, W. L.; Lim, M. H.; Reid, D. S.; Chen, H. Chemical Reaction Kinetics in Relation to Glass Transition Temperatures in Frozen Food Polymer Solutions. *J. Sci. Food*. **1993**, *61*, 51−56.

(4) Lievonen, S. M.; Laaksonen, T. J.; Roos, Y. Glass transition and reaction rates: nonenzymatic browning in glassy and liquid systems. *J. Agric. Food Chem.* **1998**, *46*, 2778−2784.

(5) Bell, L. N.; Hageman, M. J. Differentiating between the effects of water activity and glass transition dependent mobility on a solid-state chemical reaction: aspartame degradation. *J. Agric. Food Chem.* **1994**, *42*, 2398−2401.

(6) Xu, F.; Wang, Z.; Xu, S.; Sun, D.-W. Cryostability of frozen concentrated orange juices produced by enzymatic process. *J. Food Eng.* **2001**, *50*, 217−222.

(7) Roos, Y. In *Phase Transitions in Foods*; Taylor, S. L., Ed.; Academic Press: San Diego, CA, 1995.

(8) Roos, Y.; Karel, M.; Kokini, J. L. Glass Transitions in Low Moisture and Frozen Foods: Effects on Shelf Life and Quality. *Food Technol.* **1996**, Nov, 95−108.

(9) Goff, H. D. Low-temperature stability and the glassy state of frozen foods. *Food Res. Int.* **1992**, *25*, 317−325.

(10) Simatos, D.; Blond, G. DSC studies and stability of frozen foods. In *Water Relationships in Foods*; Levine, H., Slade, L., Eds.; Plenum Press: New York, 1991; pp 139−155.

(11) Reid, D. Optimizing the Quality of Frozen Foods. *Food Technol.* **1990**, July, 78−82.

(12) Levine, H.; Slade, L. Principles of "cryostabilization" technology from structure/property relationships of carbohydrate/water systems−a review. *Cryo-Lett.* **1988**, *9*, 21−63.

(13) Levine, H.; Slade, L. A Food Polymer Science Approach to the Pratice of Cryostabilization Technology. *Comments Agric. Food Chem.* **1989**, *1* (6), 315−393.

(14) Ablett, S.; Izzard, M. J.; Lillford, P. J. Differential Scanning Calorimetric Study of Frozen Sucrose and Glycerol Solutions. *J. Chem. Soc., Faraday Trans.* **1992**, *88* (6), 789−794.

(15) Roos, Y.; Karel, M. Phase Transitions of Amorphous Sucrose and Frozen Sucrose Solutions. *J. Food Sci.* **1991**, *56* (1), 266−267.

(16) Inoue, C.; Ishikawa, M. Glass Transition of Tuna Flesh at Low Temperature and Effects of Salt and Moisture. *J. Food Sci.* **1997**, *62* (3), 496−499.

(17) Levine, H.; Slade, L. Response to the letter by Simatos, Blond and Le Meste on the relation between glass transition and stability of a frozen product. *Cryo-Lett.* **1989**, *10*, 347−370.

(18) Nesvadba, P. Glass transitions in aqueous solutions and foodstuffs. In *The Glassy State in Foods*; Blanshard, J. M. V., Lillford, P. J., Eds.; Nottingham University Press: Loughborough, U.K., 1993; pp 523−526.

(19) Jensen, K. N., Danish Institute for Fisheries Research, Department of Seafood Research, University of Denmark, personal communication.

(20) Brake, N. C.; Fennema, O. R. Glass Transition Values of Muscle Tissue. *J. Food Sci.* **1999**, *64* (1), 10−15.

(21) Bai, Y.; Rahman, M. S.; Perera, C. O.; Smith, B.; Meltan, L. D. State diagram of apple slices: glass transition and freezing curves. *Food Res. Int.* **2001**, *34*, 89−95.

(22) Gill, P. S.; Sauerbrunn, S. R.; Reading, M. Modulated differential scanning calorimetry. *J. Therm. Anal.* **1993**, *40*, 931−939.

(23) Reading, M.; Luget, A.; Wilson, R. Modulated differential scanning calorimetry. *Thermochim. Acta* **1994**, 295−307.

(24) Izzard, M. J.; Ablett, S.; Lillford, P. J.; Hill, V. L.; Groves, I. F. A modulated differential scanning calorimetric study. Glass transitions occurring in sucrose solutions. *J. Therm. Anal.* **1996**, *47*, 1407−1418.

(25) Höhne, G.; Hemminger, W.; Flammersheim, H.-J. Theoretical Fundamentals of Differential Scanning Calorimeters. In *Differential Scanning Calorimetry. An Introduction for Practitioners*; Höhne, G., Hemminger, W., Flammersheim, H.-J., Eds.; Springer-Verlag: Berlin, Germany, 1996; pp 21−38.

(26) Schmidt, S. J.; Lammert, A. M. Physical Aging of Maltose Glasses. *J. Food Sci.* **1996**, *61* (5), 870−875.

(27) Roos, Y.; Karel, M. Amorphous state and delayed ice formation in sucrose solutions. *Int. J. Food Sci. Technol.* **1991**, *26*, 553−566.

(28) Sugisaki, M.; Suga, H.; Seki, S. Calorimetric Study of the Glassy State. IV. Heat Capacities of Glassy Water and Cubic Ice. *Bull. Chem. Soc. Jpn.* **1968**, *41*, 2591−2599.

(29) Johari, G. P.; Hallbrucker, A.; Mayer, E. The glass−liquid transition of hyperquenched water. *Nature* **1987**, *330* (10), 552−553.

(30) Luyet, B.; Rasmussen, D. Study by differential thermal analysis of the temperatures of instability of rapidly cooled solutions of glycerol, ethylene glycol, sucrose and glucose. *Biodynamica* **1968**, *10* (211), 167−191.

(31) Suzuki, T.; Franks, F. Solid−Liquid Phase Transitions and Amorphous States in Ternary Sucrose−Glycine−Water Systems. *J. Chem. Soc., Faraday Trans.* **1993**, *89* (17), 3283−3288.

(32) Arvanitoyannis, I.; Blanshard, J. M. V.; Ablett, S.; Izzard, M. J.; Lillford, P. J. Calorimetric Study of the Glass Transition Occurring in Aqueous Glucose:Fructose Solutions. *J. Sci. Food Agric.* **1993**, *63*, 177−188.

(33) Rockland, L. B. Saturated Salt Solutions for Static Control of Relative Humidity between 5° and 40 °C. *Anal. Chem.* **1960**, *32*, 1375−1376.

(34) Greenspan, L. Humidity Fixed Points of Binary Saturated Aqueous Solutions. *J. Res. Nat. Bur. Stand. A: Phys. Chem.* **1977**, *81A* (1), 89−96.

(35) Gordon, M.; Taylor, J. S. Ideal copolymers and the second-order transitions of synthetic rubbers. I. Non-crystalline copolymers. *J. Appl. Chem.* **1952**, *2*, 493−500.

Received for review March 22, 2002. Revised manuscript received August 16, 2002. Accepted September 19, 2002.

JF020355X